# Comparison between ORC and $CO_2$ power systems for the exploitation of low-medium temperature heat sources

Marco Astolfi [a, *], Dario Alfani [a], Silvia Lasala [b], Ennio Macchi [a]

[a] Politecnico di Milano, Dipartimento di Energia, Via Lambruschini 4, 20156 Milano, Italy
[b] Université de Lorraine, Laboratoire Réactions et Génie des Procédés, 1 Rue Grandville, 54000 Nancy, France

**ABSTRACT**

Low-medium temperature heat sources in the range 5−50 $MW_{th}$ are made available by many industrial fields but they may also be of interest for biomass, geothermal and solar energy applications. ORC has been proposed in the last 20 years as a reliable solution for the exploitation of these energy sources since the alternative represented by steam cycles leads to an inefficient conversion of such small available thermal powers. However, the use of organic fluids involves a number of safety and environmental issues, either related to fluid flammability (for hydrocarbons) or to their high Global Warming Potential (for halogenated fluids), and of limitations to the achievable cycle maximum temperature, due to fluids thermal decomposition. To overcome these limitations, in recent years $CO_2$-based transcritical and su-percritical cycles have been proposed as a viable option for this kind of applications. The present work aims to present a comparison between four $CO_2$ cycle configurations and four ORC layouts using a working fluid selected from 47 candidates. The final result is a set of performance maps that allow for an easy selection of the best solution for applications exploiting low-medium temperature heat sources.

*Keywords:*
ORC
$CO_2$
Carbon dioxide
Waste heat
recovery
Optimization
Renewable energy

## 1. Introduction

Among closed-cycle power plants the steam Rankine cycle plays a dominant role in large-scale stationary power generation. This power plant is widely used worldwide in different configurations depending on the heat source, the maximum attainable temperature and the thermal power availability. Ultra-Super Critical (USC) and future AUSC (advanced USC) are the most efficient solution and are commonly adopted for large scale (up to 1 GW) fossil fuel based applications [1,2]. Indeed, high performances are achieved by the use of steam at very high pressure (300 bar) and temperature (620 °C), which involves the use of expensive materials and justify the convenient application of these cycles to high-temperature and large-scale applications. To recover lower temperature heat sources represented for example by hot gases discharged by gas turbines (450 °C - 600 °C), subcritical superheated steam cycles without feed-water preheating represent a common solution. Improved results can be achieved adopting two or three evaporation levels plus vapor reheating as for combined cycles at the state-of-the art [3]. Subcritical steam plants are also used in large scale CSP (Concentrating Solar Power) applications based on either parabolic trough [4] or solar tower system [5−7]. Those adopt an opportune high temperature oil (390 °C) or molten salt (565 °C) [8] as Heat Transfer Fluid (HTF) in the solar field and in the storage system. Finally, saturated steam cycles with maximum temperature around 300 °C are commonly used in nuclear plants in both BWR and PWR (Boiling and Pressurized Water Reactors) configurations [9]. All the steam cycle applications mentioned above concern the exploitation of medium-high power grades (50 MW−1.5 GW).

By contrast, the low efficiency of steam Rankine cycles eventually used to exploit relatively small available thermal powers (from few hundreds of kW up to tens of MW) and/or low-medium heat source temperatures (namely between 80 and 400 °C) actually prevents the use of water as working fluid [10]. This kind of applications concern small biomass plants, small and low-temperature solar systems, small-scale industrial Waste Heat Recovery (WHR) and geothermal plants. The exploitation of low temperature heat sources by means of steam cycles would entail, in fact; the use of subcritical cycles with very low evaporation temperature and a large enough superheating grade to guarantee a sufficiently high vapour quality at turbine discharge, leading to a strong penalization of cycle thermodynamic performance. Also, steam cycles with low thermal input would involve the

* Corresponding author.
E-*mail address:* marco.astolfi@polimi.it (M. Astolfi).


Published Journal Article available at: https://doi.org/10.1016/j.energy.2018.07.099

**Nomenclature and acronyms**

| | |
|---|---|
| CR | Cascaded Recuperative |
| CSP | Concentrated Solar Power |
| ECO | Economizer |
| EVA | Evaporator |
| HRU | Heat Rejection Unit |
| HTF | Heat Transfer Fluid |
| p | Pressure |
| PHE | Primary Heat Exchanger |
| Q | Thermal Power |
| Rec | Recuperator |
| RR | Recompressed Recuperative |
| S | Specific Entropy |
| Sat-R | Saturated Recuperative |
| Sat-nR | Saturated non Recuperative |
| Sh-nR | Superheated non Recupaerative |
| $sCO_2$ | Specific entropy supercritical $CO_2$ |
| SH | Superheating |
| Sh-R | Superheated Recuperative |
| SnR | Simple non-Recuperative |
| SP | Turbine size parameter |
| SR | Simple Recuperative |
| T | Temperature |
| Vr | Turbine volume ratio |
| WHR | Waste Heat Recovery |
| $\eta$ | Efficiency |

miniaturization of the turbine still having very high enthalpy drops with a consequent reduction of the expansion isentropic efficiency and the increased component specific cost [11]. The use of a working fluid alternative to water, characterised by more appropriate thermodynamic properties, actually allows to avoid the occurrence of the aforementioned issues and to achieve higher plant efficiency. This technology generally based on the use of organic compounds (hydrocarbons, halogenated hydrocarbons, siloxanes) is named Organic Rankine Cycle (ORC) and currently represents the most reliable option available on the market for the exploitation of low-medium temperature heat sources in a large range of plant power outputs (from few kW to tens of MW). Compared to water, in fact, organic fluids enable the reduction of the evaporation pressure, the increase of the condensation one, leading to a lower number of stages and reduced costs of the turbine and, likely, to higher cycle efficiency. In the last 20 years, the ORC technology has been able to penetrate the market in a more effective way with respect to other technologies, such as the Kalina cycle and the Goswami cycle [12] or the thermoacoustic Stirling engine [13], reaching more than 2.8 GW of installed power and more than 1700 installed plants [14]. However, organic fluids suffer from low thermal stability that causes fluid cracking at temperatures around 350 °C preventing their reliable use at higher temperatures [15]. Considering the mentioned actual applications of steam cycles and ORC, it is possible to observe that there exists a spectrum of conditions in which these technologies can compete. Such a set of cases includes medium-to-high temperature heat sources and medium power outputs (from 5 MW to 20 MW). The ORC community is used to refer to such a spectrum of conditions as "**steam vs. ORC grey zone**", underling that the choice between the two power systems is by no means self-evident [10].

Another technology being able to compete with steam cycles in different applications is the closed-cycle $CO_2$ power plant which has gained, in recent years, a large interest from both the Industry and the Scientific Community [16]. Transcritical and supercritical $CO_2$ cycles are typically envisaged for large (50 MW to hundreds of MW) and high-temperature (>600 °C) power plants coupled with different thermal sources: solar energy (solar tower technology) [17], nuclear energy (IV generation nuclear reactors) [18] and fossil fuels [19,20]. In these fields of application, $CO_2$ plants can compete against conventional steam cycles thanks to their smaller investment cost, more compact turbomachines, simpler plant arrangement, higher efficiency and flexibility. A number of experimental plants have been designed and tested in recent years with a focus on solar [21,22] and nuclear applications [23,24]. A 25 MW plant is in construction in Texas with a turbine manufactured by Toshiba [25]. It is thus possible to identify another set of conditions in which steam cycles do not represent the only possibility but, conversely, an alternative to $CO_2$ cycles. In such a "**steam vs. $CO_2$ grey zone**" the choice between steam and $CO_2$ is indeed not straightforward [26–29].

Moreover, besides the already mentioned high-temperature application of $CO_2$ power cycles, this technology may be also considered as a solution for the exploitation of medium temperature heat sources comparably viable to the one represented by ORC and possibly preferred thanks to the valuable advantage of using an environmental friendly, widely available, safe and thermally stable working fluid. In the United States this concept is investigated by Echogen [30–32], which manufactures supercritical simple recuperated $CO_2$ cycles for waste heat recovery applications which operate close to the critical point, offering, in addition, efficient Combined Heat and Power solutions (CHP). Scientific literature lacks in providing a clear comparison among ORC and $CO_2$ cycles for low-medium temperatures since (i) calculations performed by different authors rely on different assumptions, (ii) ORC are rarely optimized by varying different cycle parameters and investigating several working fluids and (iii) studies on $CO_2$ power plants are more focused on large-scale and high temperature applications. This paper aims to delineate the "**ORC vs. $CO_2$ grey zone**", providing performance maps that could enable a straightforward and fair thermodynamic comparison as well as an easier selection between ORC and $CO_2$ power plants in a wide range of applications where they may compete.

In order to investigate a large range of possible applications, the analysis is carried out considering both constant and variable temperature heat sources with a maximum temperature ranging from 200 °C to 600 °C. Each point of the performance maps provided by the paper indicates the optimal efficiency of the most performant ORC or $CO_2$ power cycles, considering their most suitable configuration among those investigated.

As regards ORC, those are modelled as both saturated and superheated subcritical Rankine cycles, possibly adopting a recuperator. The use of 47 different pure working fluids in these cycles is thus compared. Concerning $CO_2$ cycles, four plant layouts are investigated: simple non-recuperative, simple recuperative, recompressed recuperative and cascade recuperative configurations. In all cases, the considered expander is a three-stage axial turbine and its efficiency is evaluated with a correlation which accounts for the effect of volume ratio (Vr) and size parameter (SP) [33].

The analysis is performed considering both high- and low-temperature heat sinks, representative of the use of, respectively, ambient air or water. In the first case, heat is rejected to the ambient with an air-cooled condenser, limiting the $CO_2$ cycle to a non-condensing Brayton configuration. In the second case, the availability of water enables cooling the $CO_2$ below its critical

temperature (31 °C), thus entailing the possibility to condensate the $CO_2$ which, consequently, allows for the less-power-consuming compression of liquid $CO_2$ as well as for the more thermodynamically favored low-temperature heat rejection.

## 2. Methodology and general assumptions

The comparison between ORC and $CO_2$ power cycles is performed in this work considering several heat sources as representative of all the possible applications where ORC and $CO_2$ power systems may compete in the low-medium temperature range (see Fig. 1-a). These applications include: (i) power plants which exploit hot geothermal brines (with a maximum temperature of 250–300 °C if Enhanced Geothermal Systems are considered); (ii) solar power plants characterized by low maximum temperature (up to 450 °C) of the HTF in solar field and small power output (up to around 20 MW); (iii) medium-small biomass fired power plants (1–5 MW); (iv) WHR applications with a wide range of possible heat sources which might differ both on the type of industrial process they originate from and on the primary engine that releases the flue gases (gas turbine or endothermic engine). All these applications differ not only in the heat source maximum temperature but also in the minimum temperature that limits the cooling of the hot stream, as detailed herein. The reinjection temperature of geothermal brines is limited by the need to prevent well depletion or scaling issues involving silica deposition on heat exchanger surfaces and pump blades. Limitations on minimum temperatures also regard CSP and biomass applications, where the diathermic oil used as HTF (into the solar field or in the biomass boiler) cannot be cooled down to very low temperature because of the necessity to avoid pouring issues or an excessive fluid viscosity, which would increase the power consumption of circulating pumps. Finally, in the case of heat recovery from flue gases, the minimum cooling temperature is generally limited to 80–150 °C to avoid the condensation of acid compounds but it can be higher if other waste heat recovery processes exploit the same hot stream.

For all the calculations, we consider heat sources characterized both by different maximum temperatures, $T_{s,max}$, (comprised between 200 °C and 600 °C) and by different cooling grades $\Delta T_{\%}$ (varying from 0 to 100%). The cooling grade is defined as the ratio between the maximum allowable temperature variation of the heat source and the maximum temperature difference given by $T_{s,max} - T_0$, where $T_0$ is the temperature of the heat sink, respectively 15 °C for water and 25 °C for ambient air. Minimum temperature of the heat source are thus calculated with the following equation, eq. (1).

$$T_{s,min} = T_{s,max} - \Delta T_{\%}(T_{s,max} - T_0) \quad (1)$$

where $T_{s,max}$, $\Delta T_{\%}$ and $T_0$ will be specified to represent specific applications.

This approach allows to investigate a wide number of cases, from completely isothermal heat sources ($\Delta T_{\%} = 0\%$) to hot streams undergoing complete cooling down to ambient temperature ($\Delta T_{\%} = 100\%$). Fig. 1-a shows the different applications investigated in this study, considering a maximum temperature of the heat source comprised between 200 °C and 600 °C. Fig. 1-b then reports the minimum temperature of the heat source, calculated as a function of $T_{s,max}$, $\Delta T_{\%}$ and $T_0 = 15°C$. Moreover, for each case-study identified by $T_{s,max}$ and $\Delta T_{\%}$, Fig. 1-c shows the plant efficiency attainable with a reversible process, namely a Carnot cycle for the exploitation of isothermal heat sources and trapezoidal or triangular Lorenz cycles for non-isothermal heat source applications. In all the treated cases, the thermal power made available by the heat source ($Q_{max}$) is fixed to 30 $MW_{th}$, representative of the small-medium power systems under comparison. For each heat source condition, identified by $T_{s,max}$ and $\Delta T_{\%}$ in each point of the grids of Fig. 1, four ORC cycle configurations and four $CO_2$ power cycle configurations are thus optimized and compared. It is worth observing that, in general, the thermal power actually entering an optimized cycle (i.e. characterized by a maximal efficiency) may be lower than the one made available by the complete cooling, from $T_{s,max}$ to $T_{s,min}$, of heat source (30 $MW_{th}$). The maximization of cycle efficiency, calculated as reported in eq. (2), depends on both the heat actually entering the cycle ($Q_{in}$) and the cycle thermodynamic efficiency. The increase of the cycle thermodynamic efficiency (by adopting recuperators in $CO_2$ cycles or by increasing the evaporation temperature in ORC systems) may lead to a non-complete exploitation of the heat source and, thus, to a reduction of the heat input to the cycle and a minimum heat source temperature higher than the one reported in Fig. 1-b.

$$\eta_{plant} = \frac{W_{el}}{Q_{max}} = \frac{Q_{in}\eta_{tdn}}{Q_{max}} \quad (2)$$

The results which have been obtained are presented as *performance maps* that present the resulting optimal configuration, among the ones considered in this work and allow for an easy comparison between ORC and $CO_2$ power systems. The analysis is repeated for two different heat sinks, either available at 15 °C (as representative of cooling water from a borehole, a river or a lake) or at 25 °C (representative of ambient air), thus resulting in the production of two performance maps. The selection of two different heat sink temperatures allows comparing ORC power systems with both supercritical $CO_2$ cycles and transcritical $CO_2$ configurations, in which $CO_2$ condensation is attainable thanks to the availability of low-temperature ($T_0 = 15$ °C) heat sinks.

Table 1 summarizes the assumptions common to ORC and $CO_2$ configurations, regarding their interaction with the heat source and

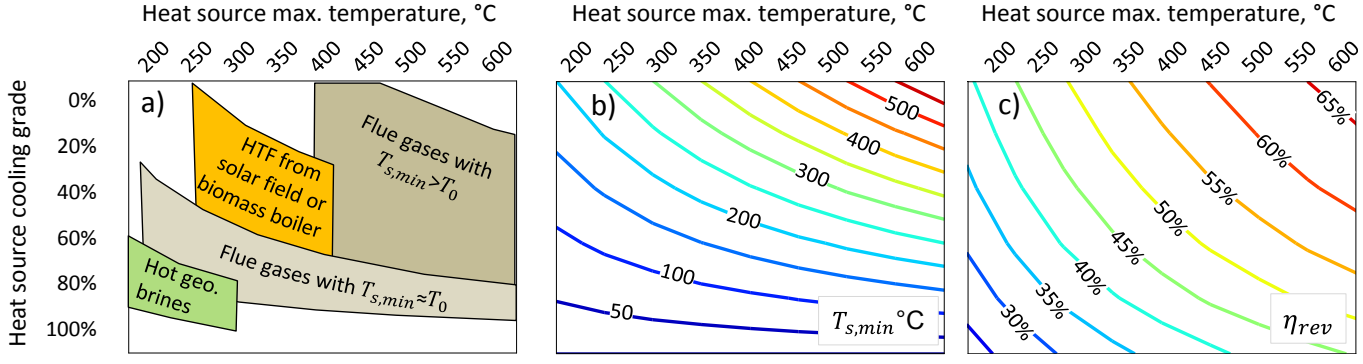


**Fig. 1.** a) Field of application of the present methodology, b) Minimum temperature of the heat source and c) Reversible cycle maximum efficiency attainable from the heat source, as a function of the maximum temperature of the heat source and of the cooling grade for water-cooled applications.

the heat sink and the design of the main components. The consumption of the Heat Rejection Unit (HRU) has been accounted differently, according to the different adopted cooling medium. For air-condensed ORC, the fan consumption is calculated as described in Ref. [34] assuming a pinch-point temperature difference in the condenser equal to 1 °C that results in a specific fan consumption equal to 0.0732 $kW/m^2_{int}$. For air-cooled $CO_2$ cycles the fan power is set equal to 0.5% of thermal power rejected to the environment, representative of the value of gas cooler consumption in refrigeration and air conditioning large scale applications [35]. In case of cooling water for both ORC and $CO_2$ cycles, the pump consumption is determined assuming a fixed temperature rise in the unit equal to 7 °C and an overall pressure drop on the water loop equal to 1.5 bar.

In the following sections 3 and 4 we describe in more details the configurations of ORC and $CO_2$ power cycles, providing the applied specific assumptions and the description of the optimization process. Each simulation has been performed in Matlab® [36] using Refprop 9.1 [37] for the calculation of thermodynamic properties.

## 3. $CO_2$ power plants

### 3.1. Plant configurations description

In $CO_2$ cycles the working fluid is compressed, heated, expanded and eventually cooled down in a closed loop configuration. In this study, four different cycle configurations are investigated starting from the simple non-recuperative cycle and moving towards solutions oriented to an increase of systems efficiency and power output. Fig. 2 depicts the four water-cooled cycles layouts and the T-s and T-Q diagrams of the optimal solutions obtained by exploiting a heat source with $T_{max}$ equal to 600 °C and cooling grade equal to 60%.

The simplest configuration (Fig. 2-a) is the simple non-recuperative (SnR) closed cycle, consisting in a compressor (or a pump) that pressurizes the $CO_2$ up to the specified cycle maximum pressure, a primary heat exchanger where the $CO_2$ is heated to the cycle maximum temperature, a turbine extracting and converting the $CO_2$ enthalpy drop into useful mechanical power and a gas cooler heat exchanger that releases heat to the ambient cooling the $CO_2$ down to the cycle minimum temperature. In spite of its simplicity and its ability to exploit heat sources with a high-cooling grade, this cycle suffers from a poor thermodynamic efficiency and requires large pressure ratios thus reducing the possibility to conveniently exploit, during compression, real gas effects in the proximity of the critical point.

The use of a recuperator in simple recuperative (SR) cycle configurations (Fig. 2-b) is generally suggested, as it reduces the optimal pressure ratio and improves cycle efficiency. The recuperator recovers a large fraction of the thermal power available at the turbine discharge, allowing the pre-heating of the compressed fluid thus leading to two main advantages: (i) a reduction of both the heat input and the heat rejected to the environment (and, consequently, a further reduction of auxiliaries power consumption) and (ii) an increase of the power output due to a larger mass flow rate of the working fluid, for a given thermal input. However, a recuperator with large heat exchange surfaces can be disadvantageous as it may reduce the grade of exploitation of the available heat source; in such a case, the pinch-point temperature difference in the recu-perator (representative of the surface of the heat exchange), $\Delta T_{pp,rec}$, should thus be optimized. However, a preliminary analysis has shown that the highest efficiency is always obtained with the smallest possible value of $\Delta T_{pp,rec}$, also for heat sources character-ized by a high cooling grade. In fact, if the recuperator is considered with its pressure drops, it is always preferable to adopt recuper-ators characterised by an extended heat exchange surface (i.e., reduced $\Delta T_{pp,rec}$), in order to reduce energy consumptions related to heat rejection unit. From an economic point of view, the intro-duction of a recuperator in a closed gas cycle generally does not involve a marked increase of capital cost (differently to open gas cycles) since the presence of this component allows to reduce the size of both the PHE and the HRU. Similar considerations also apply to the system flexibility (start-up time, load variation, etc.), strongly dependent on the thermal inertia of the heat exchangers. Moreover, Simple Recuperative (SR) $CO_2$ power cycles should conveniently operate with a minimum pressure and temperature close enough to the critical point in order to decrease the compression work, taking advantage from the remarkably lower compressibility factor (0.2−0.4) which characterises the fluid around the critical region. If real gas effects lead to the reduction of the power required for pressurization on one side, those represent, on the other side, a limit for the efficacy of the recuperator in the simple recuperative cycle (SR). The difference in the specific heat capacities of $CO_2$ between the low temperature and high pressure cold side of the recuperator and the higher temperature and lower pressure hot one leads to relevant temperature difference between the two sides of the recuperator (see the T-Q diagram in Fig. 2-b) and a more irreversible heat transfer process.

In order to mitigate this penalization, the recompressed recuperative cycle (RR) (Fig. 2-c), originally proposed by Angelino [38], has also been considered in this work. Differently from the simple recuperative (SR) cycle configuration, the internal recovery process of the recompressed cycle takes place in two different heat

**Table 1**
General assumptions for ORC and $CO_2$ configurations.

| | $CO_2$ | | ORC | |
|---|---|---|---|---|
| Heat sink temperature | 15 °C water cooled | 25 °C air cooled | 15 °C water cooled | 25 °C air cooled |
| Minimum working fluid temperature | 25 °C | 40 °C | 25 °C | 40 °C |
| $\Delta T_{ap,PHE}$, $\Delta T_{pp,\ PHE}$, $\Delta T_{pprec}$ | 10 °C | | 5 °C | |
| $\Delta T_{subcooling}$ | – | | 5 °C | |
| Δp (or, whether relative, $\Delta p/p_{in}$) PHE | 2% | | 50 kPa (ECO), ΔT = 1 °C (EVA), 2% (SH) | |
| Δp (or, whether relative, $\Delta p/p_{in}$) REC | 2% (hot side), 2% (cold side) | | 2% (hot side), 50 kPa (cold side) | |
| Δp (or, whether relative, $\Delta p/p_{in}$) HR | 2% | | 2% (desuperheating), ΔT = 0.5 °C (condensation) | |
| Compressor/pump hydraulic efficiency | 0.85 | | 0.75 | |
| Generator electrical efficiency | 0.97 | | | |
| Mechanical efficiency | 0.97 | | | |
| Pump electrical motor efficiency | 0.97 | – | 0.97 | |

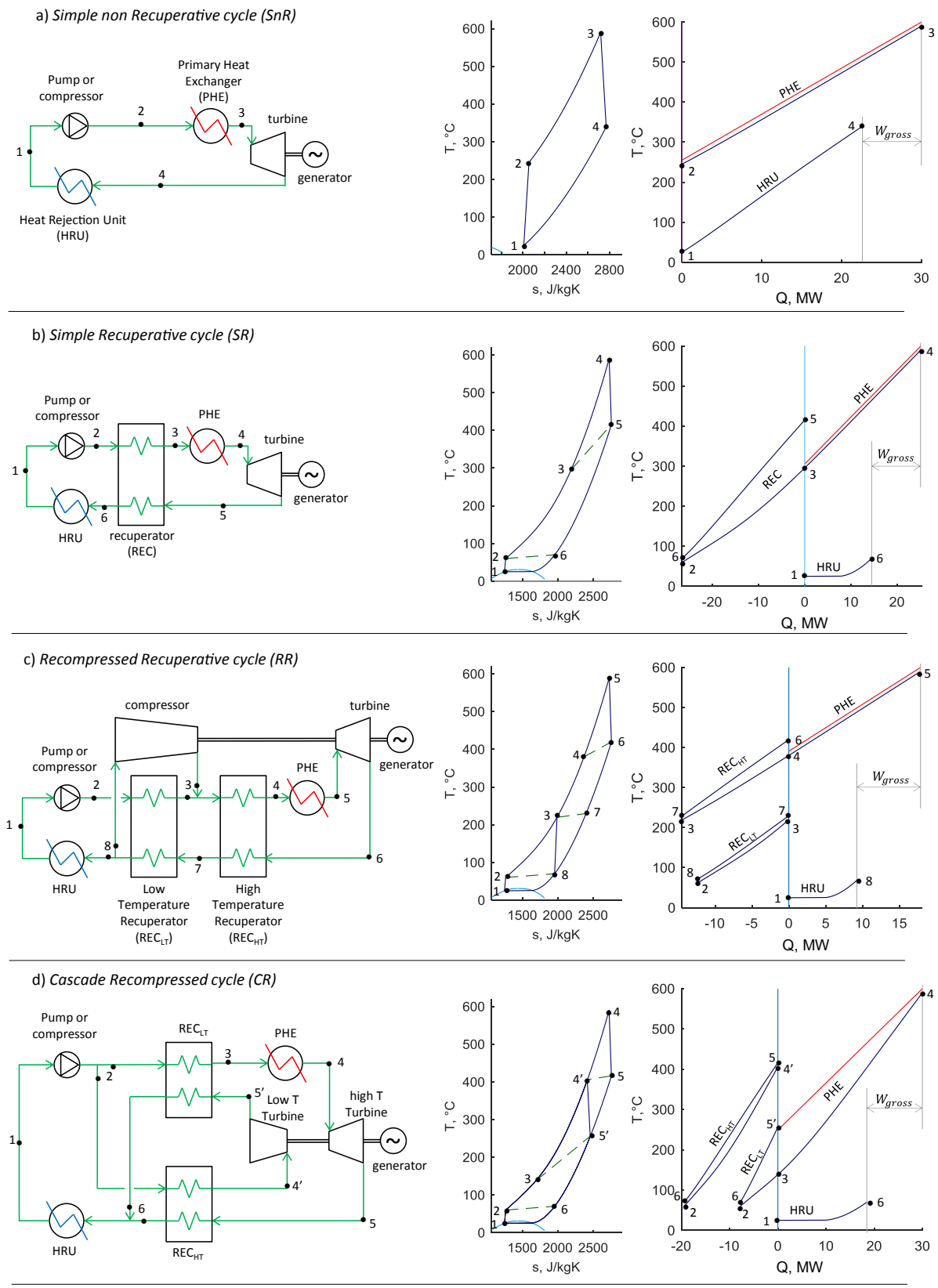


**Fig. 2.** Plant layout, T-s and T-Q diagrams for the four $CO_2$ cycle configurations under investigation.

exchangers. The cold and high-pressure side of the low-temperature recuperator is characterized by a reduced $CO_2$ mass flow rate to better balance the heat capacities of the hot and cold recuperator sides, in order to reduce the average temperature difference between the two streams and, thus, increase the cycle efficiency. The remaining portion of the low-pressure $CO_2$ which bypasses the HRU is pressurized in a separate compressor and then reinjected in the main stream at the outlet of the low-temperature recuperator. As already mentioned, the main drawback of optimized recuperative configurations, especially the recompressed one (RR), is related to the very high mean temperature of the heat introduction process which limits the exploitation of heat sources featuring a high cooling grade. To efficiently exploit this kind of heat sources it is crucial to find the best trade-off between the increase of cycle thermodynamic efficiency and the reduction of heat input.

A possible proposed solution is represented by the adoption of the cascade recuperative cycle (CR) [39]. In this cycle configuration (Fig. 2-d), the $CO_2$ mass flow rate is split just after the pump unit: the main stream after a preheating is heated up to the maximum cycle temperature in the PHE while the secondary stream is heated by a recuperator which recovers the heat available at the discharge of the high-temperature turbine. The heat available after the low-temperature turbine is partially recovered to preheat the main stream in a second recuperator. As a result, this cycle is characterised by a lower efficiency with respect to the one of the optimal recompressed recuperative cycle, but it enables a more complete exploitation of variable temperature heat sources.

In case of water-cooled cycle, the $CO_2$ plant is condensative while, for the air-cooled configuration, the cycle minimum temperature is above the critical temperature of $CO_2$, thus resulting in a supercritical configuration which adopts a compressor (directly connected to the turbine shaft) instead of a pump for working fluid compression.

### 3.2. Optimization methodology and results

The optimal design of each configuration is the one that maximises the plant efficiency and hence the power output. The set of optimizing variables changes depending on the cycle configuration and the available heat sink. The maximum pressure of the cycle is optimized at all times (considering an upper bound equal to 300 bar) as well as the minimum pressure in case of non-condensing cycles. When water is used as cooling medium, both condensing and non-condensing cycles are evaluated. In addition, also the split ratio is optimized for recompressed recuperative (RR) and cascade recuperative (CR) cycles. Turbine efficiency is computed with the equation presented in Ref. [33] as function of the turbine Size Parameter (SP) and of the volume ratio ($V_r$), considering a three-stage axial turbine. This correlation allows considering the effects of both turbine dimension and expansion volume ratio on the machine isentropic efficiency. The smaller is the turbine dimension (low SP) the higher is the efficiency penal-ization due to secondary and leakage losses. On the other hand, the higher is the volume ratio (Vr), the lower is the maximum attainable efficiency because of the difficulties in handling large volume flow rates variations in few stages, presence of supersonic velocities, large flaring angles and high stage loading. For the calculation of plants power output, we considered the compressors as connected to the turbine shaft and the pump, which is present in case of condensative water-cooled cases, as connected to an electrical motor.

A first analysis is carried out considering different $CO_2$ water-cooled configurations. In water-cooled $CO_2$ cycles, $CO_2$ can condensate at cycle minimum temperature leading to a reduced pump consumption and to an increased plant efficiency.

Fig. 3-a shows the efficiency of the optimal simple non-recuperative (SnR) $CO_2$ cycle. The power output increases with the maximum temperature of the heat source, as a result of the larger difference between turbine production and pump con-sumption for a given pressure ratio. It is interesting to note that for low maximum temperature of the heat source and high cooling grades, the optimal pressure ratio of a closed gas cycle is small resulting in a condensing optimal cycle configuration. On the contrary, for higher temperature heat sources, the optimal pressure ratio for a non-recuperative gas cycle is higher than the ratio be-tween the maximum pressure upper bound and the saturation pressure at 25 °C, resulting in an optimal non-condensing cycle. In these cases, it is preferable to increase the cycle pressure ratio instead of exploiting the real gas effects during compression. Heat source conditions for which the non-condensing cycle results more efficient than the condensing one are represented by the black solid line in Fig. 3-a. Improved efficiencies can be attained with the simple recuperative (SR) cycle (Fig. 3-b) which is more efficient than the simple non recuperative (SnR) cycle at all times except for low-temperature heat sources characterised by a high cooling grades. In such cases, in fact, the heat recovered in SR recuperator is

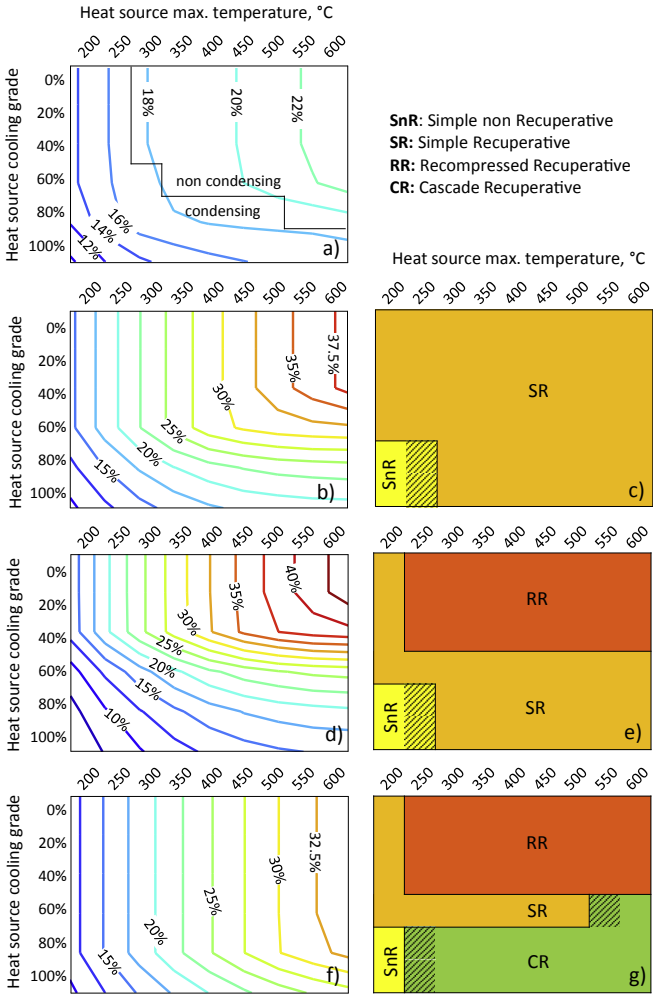


**Fig. 3.** Maximum attainable efficiency for the Simple non Recuperative (SnR) cycle (a), Simple Recuperative (SR) cycle (b), Recompressed Recuperative (RR) cycle (d) and Cascade Recuperative (CR) cycle (f) as function of heat source maximum temperature and cooling grade. Selections maps for $CO_2$ cycles: SnR vs SR (c), SR vs RR (e) and CR vs SR (g).

reduced and recuperator pressure drops contribute to the reduction of cycle efficiencies (Fig. 3-c). Recompressed recuperative cycles (RR) are more efficient than simple recuperative ones (SR) for heat source temperatures higher than 250 °C and a cooling grade lower than 40%, as shown by Fig. 3-d and Fig. 3-e. Finally, cascade recuperative cycles (CR) (Fig. 3-f and Fig. 3-g) are recommended for high cooling grade heat sources since they perform better than SR and RR cycles. In Fig. 3-c-e-g, regions where the performance of two adjacent plant configurations differ by less than 2.5% are highlighted with a line pattern. Fig. 4 shows the variation of the efficiency and power output of the four configurations as a function of the heat source cooling grade, considering a maximum temperature of the heat source equal to 450 °C. In particular, Fig. 4 highlights that the recompressed recuperative cycle (RR) dominates at low cooling grade while the cascade recuperative cycle (CR) is the most promising solution when the heat source can be cooled down to low temperature. The trend of efficiencies reveals a maximum value when the heat source results to be completely exploited.

The same comparison has been performed with air-cooled cycles and results are reported in Fig. 5. Similar conclusions as for the water-cooled cycles can be drawn.

## 4. ORC plants

### *4.1. Plant configurations description*

Two decisional variables mainly affect the design of an ORC: (i) the selection of the working fluid and (ii) the cycle configuration. However, those participate in a correlated way to the definition of the optimal cycle and must be, thus, selected simultaneously: the working fluid, which fixes the thermodynamic backbone of the cycle, influences the design of each component; vice versa, the preferable utilization of one or the other configuration may lead to the selection of one or the other working fluid. In particular:

- the critical temperature of the fluid affects in a relevant way the pressure levels within the cycle. High critical temperatures involve low pressures at both evaporation and condensation levels and an increase of turbine pressure ratio and volume ratio; this is detrimental for the application of large size ORCs which, on one side, involves issues related to the presence of non-condensable gas leakages and, on the other, requires an increase of turbine number of stages, diameter and cost [40]. On the contrary, the use of high critical temperature fluids in small size applications allows to design a compact, but not miniaturized, turbine characterized by a good efficiency;
- the fluid molecular complexity mainly affects the shape of the saturation boundaries (Andrews diagram) which separate, in a T-s diagrams, the two-phase region from the single-phase ones. In particular, increasing the molecular complexity leads to an enhanced steepness of the saturation vapor curve that becomes overhanging for highly complex fluids. Complex fluids thus positively present dry expansions even starting from saturated vapor conditions, resulting in improved turbine efficiency and lifetime. In addition, a high molecular complexity leads to small temperature drops in expansion, which involve higher temperatures of the fluid at the turbine outlet thus enabling, by means of a recuperative cycle configuration, to preheat the compressed liquid and to increase cycle efficiency.
- molecular mass also plays an important role in the assessment of component design. Higher molecular mass involves the reduction of both enthalpy drops during expansion and fluid speed of sound, leading to turbines with a reduced number of stages, low loading coefficients but supersonic velocities triangles and the need of non-conventional blade design.

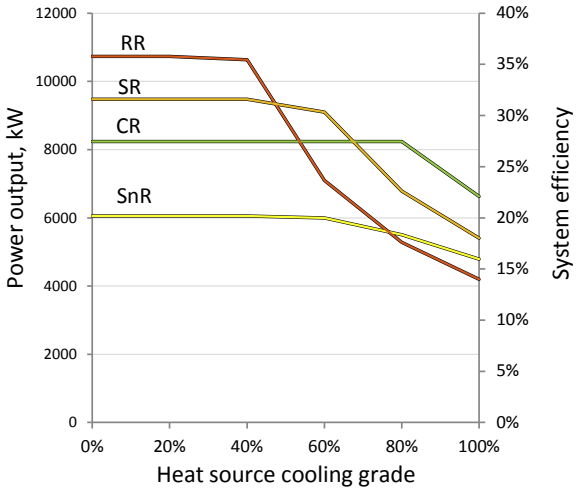


**Fig. 4.** Maximum attainable efficiency of the four $CO_2$ cycle configurations as function of the heat source cooling grade for a heat source maximum temperature equal to 450 °C.

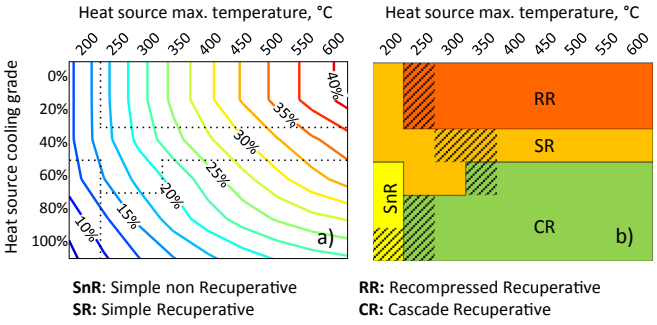


**Fig. 5.** (a) Maximum efficiency attainable with air-cooled $CO_2$ plants using the best cycle configuration among the four types investigated along the study (b).

In this work, the use of 47 potential working fluids is investigated. Thermodynamic calculations are performed with the property package made available by Refprop 9.1 [37]. Among these 47 working fluids, there are 23 hydrocarbons, among which 15 are alkanes, 16 halogenated fluids (with hydrogen atoms partially or totally substituted by fluorine atoms) and 8 siloxanes. The set of candidate working fluids spans from low critical temperature and relatively low complexity fluids (R143a, propane, R134a) up to heavy, complex and high critical temperature compounds (benzene, MDM, decane). The complete list of considered fluids is reported in Fig. 6 with their critical parameters and maximum operating temperatures. This last property is dictated by the thermal stability limit of the fluid, above which it starts to decompose in lighter compounds that change the fluid thermodynamic properties, possibly leading to the detrimental formation of solid particles that would damage the turbine blades and increase fouling on the surfaces of the heat exchangers. For each specific fluid, we consider this limit as the maximum temperature of the experimental dataset used to calibrate the equation of state.

Regarding the ORC plant configurations, the analysis is limited to subcritical cycles since the vast majority of the installed ORC plants is based on this cycle layout. Despite supercritical and two pressure levels ORCs may also be advantageous, these cycles have not been considered here since it has only been used in a limited

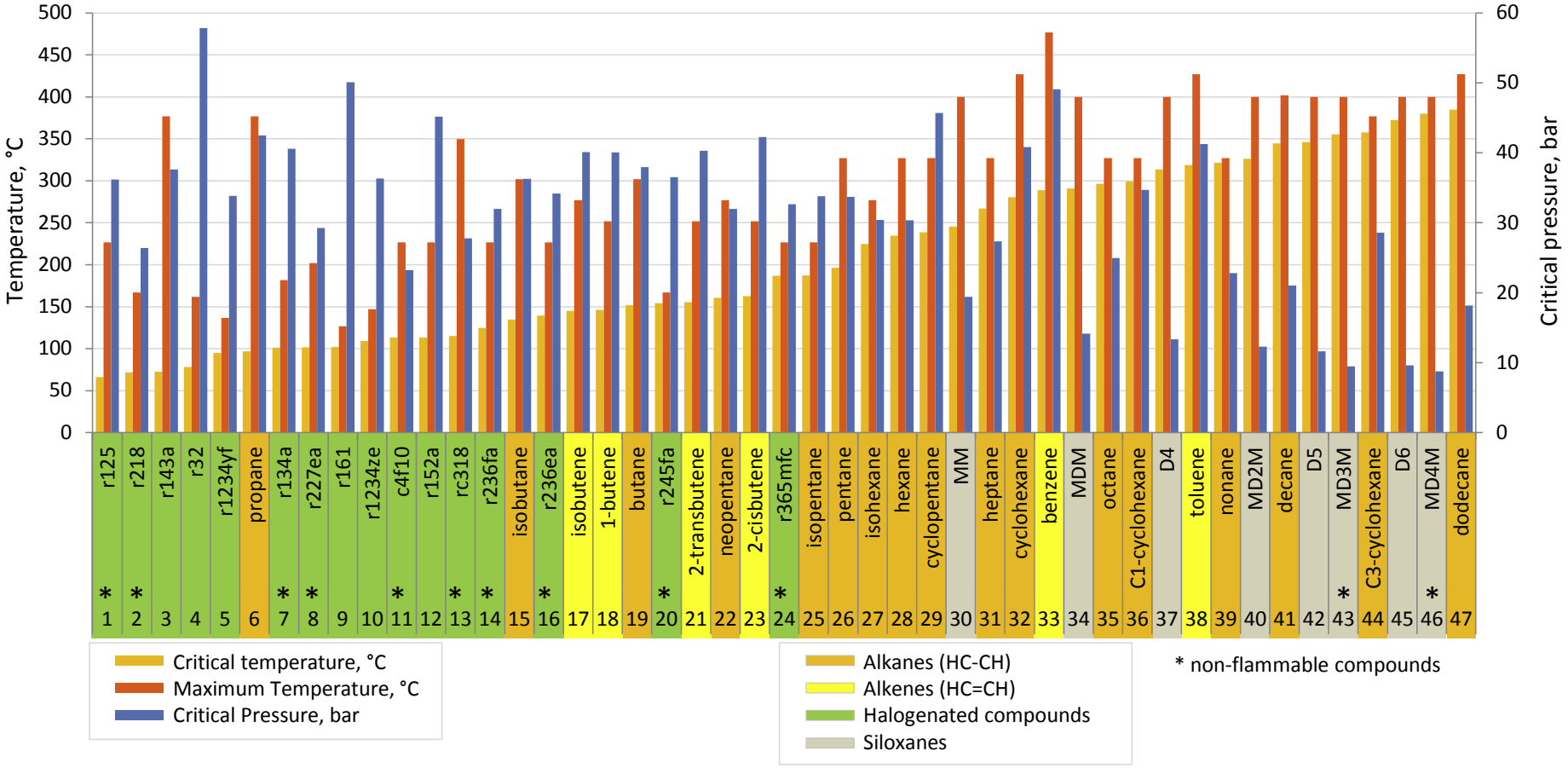


**Fig. 6.** List of the 47 working fluid candidates for ORC applications sorted from lower to higher critical temperature fluid and divided in 4 groups. Fluids labelled with (*) are non-flammable.

number of plants. Examples of supercritical cycles are the geothermal installations by TAS in USA [41], the experimental activity carried out by ENEL in Livorno [42] or in very few waste heat recovery applications. Two evaporation levels cycles are instead adopted by Exergy for the exploitation of low temperature geothermal brines [43,44]. We decided to focus this work on configurations being well-established in the current state-of-the-art of the ORC technology, based on either superheated or saturated cycles possibly provided with a recuperator. The considered general plant layout is reported in Fig. 7, together with the T-s diagram of ORC operating with butane as working fluid and corresponding to the optimal cycles for air cooled applications, which exploit a 200 °C heat source with a 40% cooling grade.

### 4.2. Optimization methodology and results

Each plant is optimized from a thermodynamic perspective varying: (i) the evaporation temperature, (ii) the condensation temperature and, only for superheated cycles, (iii) the superheating degree. Turbine efficiency is computed with the correlation presented in Ref. [33] as function of turbine SP and $V_r$, considering a three stages axial turbine, as for $CO_2$-cycles.

For complex molecules having an overhanging saturation vapor line, the maximum evaporation temperature for saturated cycles coincides with the temperature corresponding to the maximum saturated vapor entropy, in order to avoid two-phase flow expansion in the first turbine stage. Differently, for superheated cycles, the maximum evaporation temperature is set 10 °C below the critical temperature and a minimum value of superheating is imposed to 5 °C.

In case of simpler molecules characterized by non-overhanging saturation vapor lines, we consider a penalization of turbine efficiency due to the possible presence of liquid droplets: for vapor quality below 0.95 we accounted for 1 percentage point of penalization for each 1 percentage point of liquid fraction. To prevent from air leakages resulting from the achievement of subatmospheric minimum pressures by the organic working fluid, the minimum condenser pressure is limited to 1 bar. It is recalled that, in ORC, the removal of non-condensable gases by venting them in the environment is not possible by using a deaerator like in steam cycles, for safety, environmental and economic reasons. This constraint penalizes especially high-critical temperature fluids that result to be bounded to high condensing temperature. To quantify the power production lost by the imposition of such a limit, the effect of lower bound condensing pressures on ORC efficiency is discussed.

Fig. 8-a shows the maximum efficiency attainable with ORC water-cooled power plants: net power ranges from 3.6 MW to 9.5 MW respectively for low-temperature heat sources with high temperature grades and for isothermal heat sources with temperatures higher than 500 °C. Fig. 8-b depicts the best cycle layout that is always the superheated recuperative (Sh-R) one, except for low temperature heat sources having a high cooling grade. In these cases, in fact, the saturated cycle is the most efficient solution. Heat source conditions with a power production gap between saturated and superheated cycles lower than 2.5% are marked with a line pattern meaning that also saturated cycles are appropriate in these cases since they guarantee a good matching with the heat source. Finally, for heat sources with low maximum temperature and high cooling degree, the use of the recuperator is not strictly recommended since the power output results to be slightly higher than the non-recuperative cycle. An asterisk labels the heat source conditions for which the difference between the power production of the best recuperative and the best non-recuperative cycle is lower than 2.5%. The optimal working fluid is reported in Fig. 8-c: the higher the maximum average temperature of the heat source (namely high-$T_{s,max}$ and low-$\Delta T_{\%}$), the higher the critical temperature of the optimal fluid. On the contrary, for heat sources with higher temperature variations, it is preferable to adopt fluids with a lower critical temperature because they allow condensing at low temperatures while maintaining limited volume ratios and high turbine efficiency. For maximum temperatures of the heat source higher than 500 °C, the optimal ORC plant does not change as well as the system efficiency, since the maximum temperature of the cycle is bounded by the thermal stability limit of the fluid, rather than by the heat source temperature profile.

Similar results are obtained for air-cooled power plants, which prove to be characterized by a lower power production for low critical temperature fluids, according to the higher condensation temperature. The higher penalization on cycle efficiency (up to 2.3 efficiency points) is obtained for low maximum temperature and high cooling degree heat sources, as reported in Fig. 9-a. On the contrary, for high critical temperature fluids the condensation temperature is limited by the constraint on minimum condensation

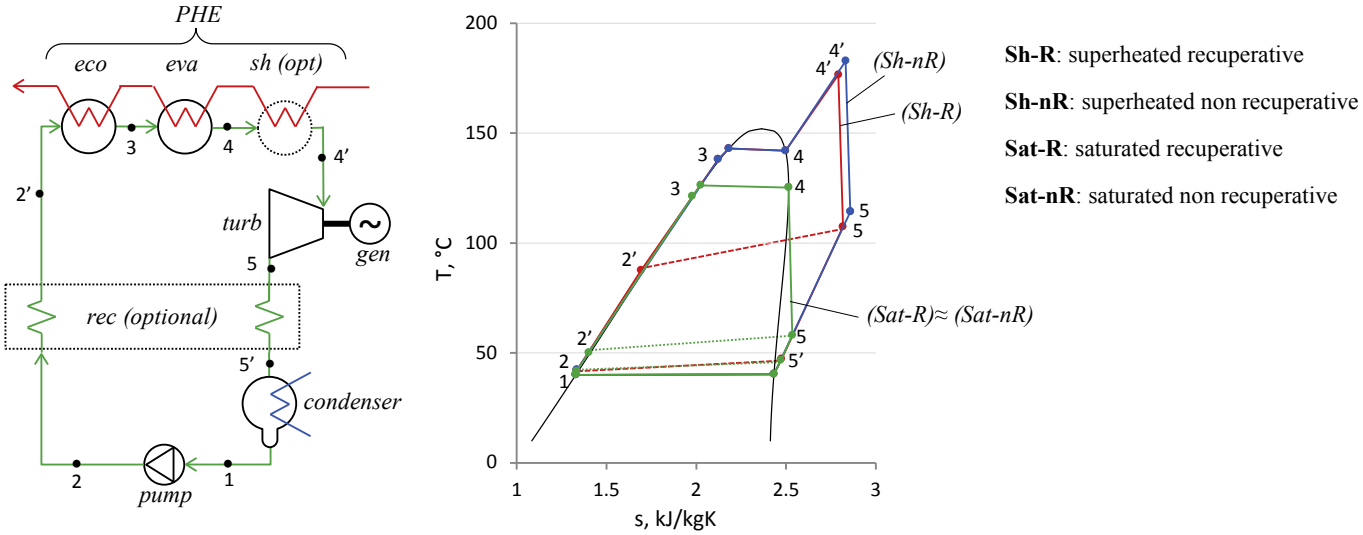


**Fig. 7.** General plant layout for ORC power systems and Ts diagram for the four cycle configurations optimized for the exploitation of an heat source having maximum temperature equal to 200 °C and cooling grade equal to 40% using butane as working fluid.

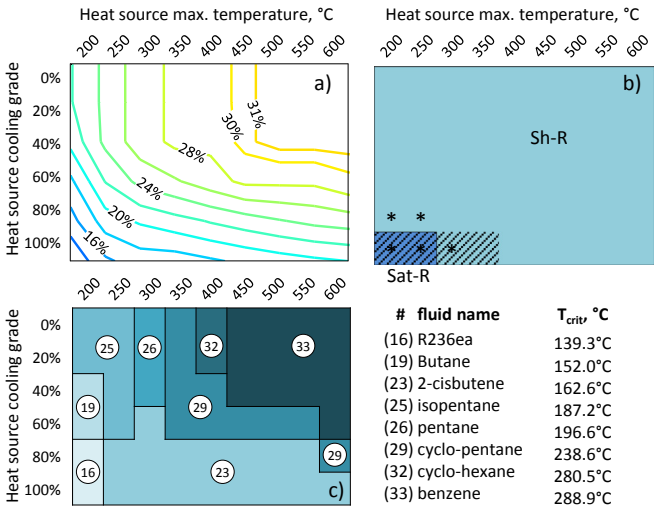


**Fig. 8.** (a) Maximum attainable efficiency with the best ORC power systems in water cooled case, (b) optimal cycle configuration (shaded area: Sat ≈ Sh, *: Rec ≈ non Rec), (c) optimal working fluid.

pressure, higher than 1bar. Optimal fluids are almost unchanged and superheated recuperative cycles are always the best option although saturated and non-recuperative cycles are interesting for low-temperature applications.

In order to highlight the effect of condensation pressure limit, an additional case is investigated setting the lower bound of this quantity equal to 0.05 bar (a typical value for steam power plant), rather than 1 bar. In this case, the use of a common deaerator is ruled out since organic fluids cannot be vented into the environment. Generally a vacuum pump is adopted to remove the non-condensable gases from the condenser, followed by a gas treatment unit in order to recover part of the organic fluid and reinsert it into the working cycle [45]. The efficiency increases for both water-cooled and air-cooled cycles as reported in Fig. 9-b and Fig. 9-c respectively. No changes in efficiency are observed for low-temperature heat sources because the limit on condensation temperature, dictated by the cooling medium temperature and the assumed value of $\Delta T_{ap,cond}$, is more restrictive than the constraint on condensation pressure.

Most of the organic fluids are either toxic or flammable and, consequently, their use typically leads to environmental and safety issues and additional cost for hazard prevention. On the contrary, $CO_2$ is a safe fluid that can be preferable in industrial and civil applications. To provide an additional comparison, which accounts for such quality parameters of organic fluids, a last analysis is performed limiting it to the use of safe organic fluids labelled with an asterisk in Fig. 6. These constraints strongly limit the number of utilizable fluids and, thus, lead to a marked reduction of obtainable power outputs. The maximum attainable efficiency (Fig. 10) is obtained with supercritical recuperative cycles working with R245fa or R236ea: two fluids having a similar critical temperature, a similar molecular formula and, thus, a similar molecular mass and complexity ($CF_3$-$CH_2$-$CHF_2$ vs $CF_3$-CHF-$CHF_2$).

## 5. Comparison ORC vs $CO_2$

The comparison of ORC and $CO_2$ *performance maps* presented in sections 3 and 4 has led to the definition of additional maps, which enable the easier assessment of the maximum efficiency attainable either with ORC power plants or with $CO_2$ cycles for all the considered conditions. Those are shown in Fig. 11 where areas with line pattern highlight the heat sources conditions that result in a difference in power production of ORC and $CO_2$ lower than the 2.5%. More details are specified in the following.

The first comparison is carried out between $CO_2$ cycles and ORC, considering a condensation pressure limit equal to 1 bar in order to avoid non-condensable gas leakage during operation. If water is available as cooling medium (Fig. 11-a), ORC proves to be preferable to $CO_2$ cycles for low-temperature heat sources (namely below 300 °C-350 °C). These cases are representative of biomass plants, solar power technologies, where a loop of synthetic oil is used within the furnace or in the solar field with temperatures usually ranging from 150 °C to 350 °C, and of cycles applied to exploit hot geothermal brines. On the contrary, $CO_2$ cycles are promising for higher-temperature heat sources. The introduction of the cascade recuperative cycle (CR) makes $CO_2$ very promising also for heat sources with a high cooling grade. $CO_2$ cycles can find application in waste heat recovery form industrial processes or from gas turbines or endothermic engines flue gases. Both ORC and $CO_2$ air-cooled plants (Fig. 11-b) are characterized by reduced performances with respect to water-cooled solutions. However, the necessary use of supercritical $CO_2$ cycles, when air is available as cooling medium, enhances their penalization with respect to the one afflicting ORC, confining $CO_2$ plants in a narrower region of the provided performance maps and highlighting the large advantages in adopting transcritical $CO_2$ cycles instead of supercritical ones.

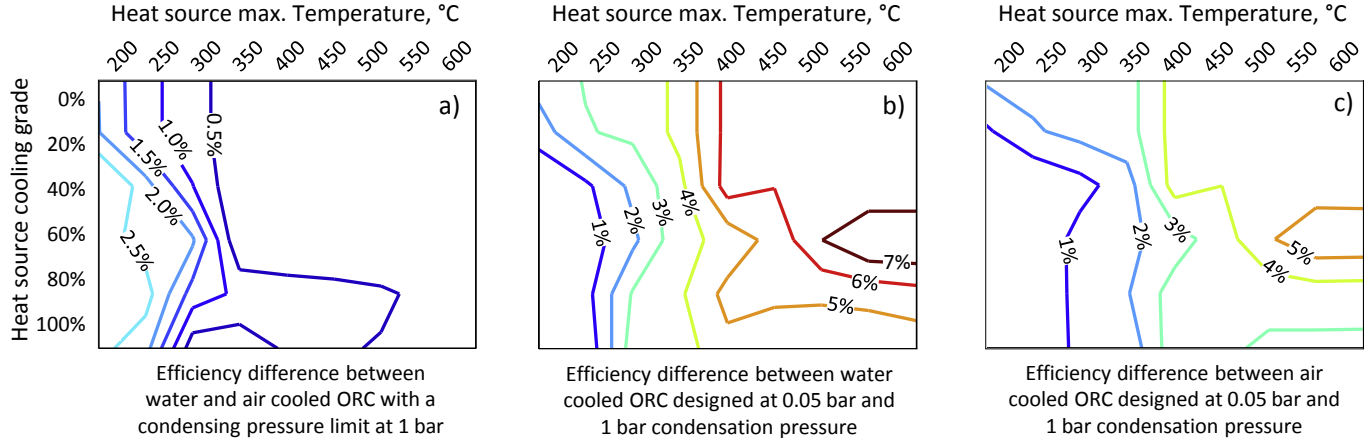


**Fig. 9.** Efficiency difference between: (a) water and air cooled ORC with pcond>1bar, (b) water cooled ORC with pcond>1 bar vs pcond>0.05 bar, (c) air cooled ORC with pcond>1 bar vs pcond>0.05.

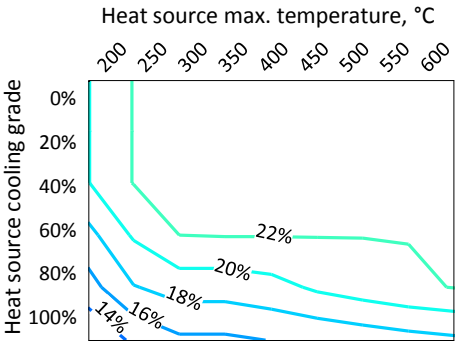


**Fig. 10.** Maximum attainable efficiency with water cooled ORC using non flammable fluids.

The second comparison is carried out considering a lower value of the minimum condensation pressure for ORC (0.05 bar instead of 1 bar), leading to the possibility to design cycles having a larger temperature difference and higher critical temperature fluids. ORC power output increases especially for systems designed to exploit high temperature heat sources; however, it is worth observing that, in these cases, the plant requires higher investment and O&M costs to limit the presence of non-condensable gases during operation. As result, the range of possible application of ORC is wider than in the previous comparison and the efficient use of $CO_2$ cycles results to interest only high temperatures heat sources.

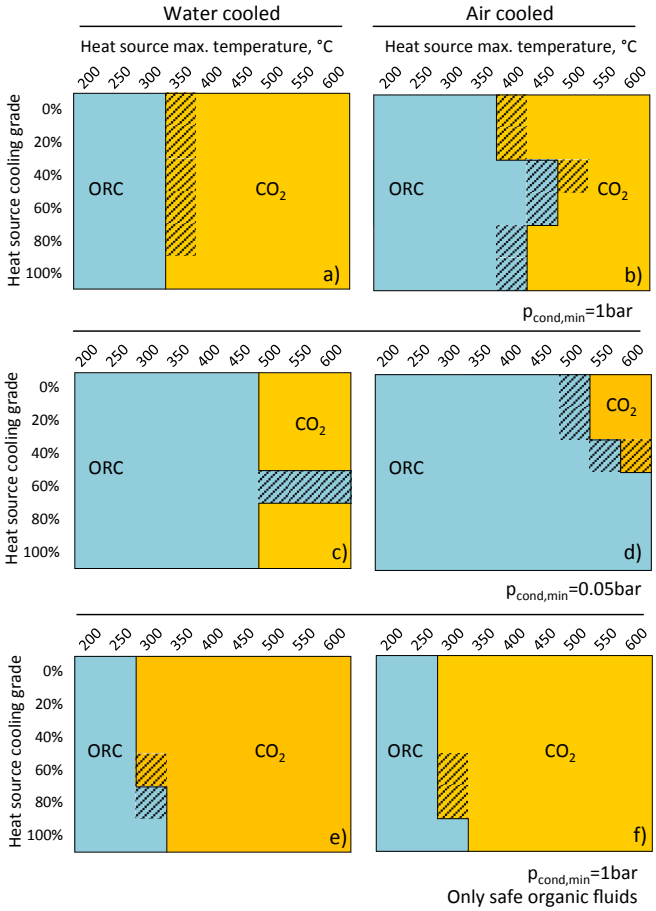


**Fig. 11.** Selection maps ORC vs $CO_2$ for water cooled and air cooled power systems in three different cases: a-b ORC with pcond>1bar, c-d ORC with pcond>0.05bar, e-f ORC with pcond>1bar and non-flammable fluids.

The last comparison is performed excluding flammable molecules from ORC candidate working fluids. In this case, $CO_2$ becomes a more interesting solution pushing the boundary of ORC applications towards lower heat source temperatures. ORC, however, still remains the best options for applications with a maximum temperature lower than 300 °C.

## 6. Conclusions

This work aims to compare performances of $CO_2$ power cycles and ORC for waste heat recovery applications. Performance maps are presented for both solutions, considering (1) heat sources characterized by different maximum temperatures ($T_{s,max} = [200\,°C – 600\,°C]$) and cooling grades ($\Delta T_{\%} = [0 – 100]$), (2) water-cooled ($T_c = 15\,°C$) and air-cooled ($T_c = 25\,°C$) cycles. The key-points of the analysis and main outcomes are briefly described below.

- In this work, $CO_2$ cycles have been designed as (i) Simple non-Recuperative (SnR), simple recuperative (SR), Recompressed Recuperative (RR) and Cascade Recuperative (CR) configurations, since they are recognized as the simplest and possibly the most suitable configurations for small to medium size plants. From the analysis it results that increasing cycle maximum pressure and temperature is profitable at all times while the cycle minimum pressure must be optimized considering the effect on both turbine efficiency and compressor consumption.
- ORC plants can be designed according to different plant layouts and they can adopt a large number of working fluids. Optimization of both aspects is crucial to obtain high conversion efficiency and to maximize power output. From the analysis reported in this paper, superheated recuperative cycles turn out to be the best solution for almost all the investigated cases with the exception of heat sources having a very high cooling grade. On the other hand, the optimal fluid critical temperature results to be strictly linked to the thermodynamic quality of the heat source.
- ORCs are the most efficient solution in a large range of applications, especially for heat source temperature below 350 °C, while $CO_2$ represents the most convenient solution for higher temperatures. The availability of cooling water leads to an improvement of the $CO_2$ efficiency thanks to the possible adoption of condensing cycles which enable the strong reduction of power consumption of the pressurization system and of HRU auxiliaries.
- Two other aspects are highlighted:
  - considering a higher vacuum at ORC condenser allows to increase the performance of these cycles, weakening even more the competitiveness of $CO_2$ systems but leading to a more complex ORC unit operation because of the need to extract non-condensable gases,
  - excluding flammable fluids from the optimization of ORC systems makes $CO_2$ cycles the preferable solution even for heat source temperature higher than 300 °C. However, $CO_2$ cycles must deal with very high pressures that make the design of the components non-trivial and also lead to safety issues.
- Finally, it is worth to underlining that, for all the cases investigated, ORC technology might compete with $CO_2$ cycles also at higher temperatures if more efficient cycle layouts were considered, such as the supercritical or the two evaporation level configurations.

## References

[1] Di Gianfrancesco A. Materials for ultra-supercritical and advanced ultra-supercritical power plants. Elsevier Science; 2016.

[2] Okita N, Sasaki T, Suga T, Iwai S. Development and strategy for a-USC steam turbine cycle. In: Proc. ASME turbo expo 2011; Jan. 2011. p. 2321–5.

[3] Lozza G. Bottoming steam cycles for combined gas-steam power plants. A theoretical estimation of steam turbine performances and cycle analysis. In: American society of mechanical engineers, vol. 5. International Gas Turbine Institute (Publication) IGTI; 1990. p. 83–92.

[4] Giostri A, Binotti M, Astolfi M, Silva P, Macchi E, Manzolini G. Comparison of different solar plants based on parabolic trough technology. Sol Energy May 2012;86(5):1208–21.

[5] Bright Source, "Ivanpah Solar Electric Generating System." [Online]. Available: http://www.ivanpahsolar.com/. [Accessed: 12-Feb-2018].

[6] Ben-Zvi R, Epstein M, Segal A. Simulation of an integrated steam generator for solar tower. Sol Energy Jan. 2012;86(1):578–92.

[7] Singer C, Buck R, Pitz-Paal R, Müller-Steinhagen H. Assessment of solar power tower driven ultrasupercritical steam cycles applying tubular central receivers with varied heat transfer media. J Sol Energy Eng Nov. 2010;132(4):041010.

[8] González-Roubaud E, Pérez-Osorio D, Prieto C. Review of commercial thermal energy storage in concentrated solar power plants: steam vs. molten salts. In: Renewable and sustainable energy reviews, vol. 80. Pergamon; 01-Dec. p. 133–48.

[9] Murray RL, Holbert KE. Nuclear power plants. Nucl Energy 2015:291–313.

[10] Macchi E, Astolfi M. Organic Rankine Cycle (ORC) Power Systems: Technologies and Applications. 1st Edition. Woodhead Publishing; 2016, ISBN 9780081005101.

[11] Macchi E. Theoretical basis of the Organic Rankine Cycle. In: Organic Rankine Cycle (ORC) power systems: Technologies and applications. 1st Edition. Woodhead Publishing; 2016, ISBN 9780081005101. p. 3–24. https://doi.org/10.1016/B978-0-08-100510-1.00001-6.

[12] Karimi MN, Dutta A, Kaushik A, Bansal H, Haque SZ. A review of organic rankine, Kalina and Goswami cycle. Int. J. Eng. Technol. Manag. Appl. Sci. 2015;3(October):2349–4476. www.ijetmas.com.

[13] Backhaus S, Swift GW. A thermoacoustic-Stirling heat engine: detailed study. J Acoust Soc Am May 2000;107(6):3148–66.

[14] Tartière T, Astolfi M. A world overview of the organic rankine cycle market. In: Energy procedia, vol. 129; 2017. p. 2–9.

[15] Invernizzi CM, Bonalumi D. 05 – thermal stability of organic fluids for Organic Rankine Cycle systems. 2017.

[16] Crespi F, Gavagnin G, Sánchez D, Martínez GS. Supercritical carbon dioxide cycles for power generation: a review. Appl Energy 2017;195:152–83.

[17] Binotti M, Astolfi M, Campanari S, Manzolini G, Silva P. Preliminary assessment of sCO2cycles for power generation in CSP solar tower plants. Appl Energy Oct. 2017;204:1007–17.

[18] Dostal V, Driscoll MJ, Hejzlar P. A supercritical carbon dioxide cycle for next generation nuclear reactors. In: Tech. Rep; 2004. p. 1–317. MIT-ANP-TR-100.

[19] Mecheri M, Le Moullec Y. Supercritical CO2 Brayton cycles for coal-fired power plants. Energy 2016;103:758–71.

[20] Allam RJ, Fetvedt JE, Forrest BA, Freed DA. The oxy-fuel, supercritical CO2 allam cycle: new cycle developments to produce even lower-cost electricity from fossil fuels without atmospheric emissions. In: ASME turbo expo 2014: turbine technical conference and exposition; 2014.

[21] Nrel. 10-MW supercritical-CO2 turbine. 2012. no. September 2012.

[22] Turchi CS, Ma Z, Neises TW, Wagner MJ. Thermodynamic study of advanced supercritical carbon dioxide power cycles for concentrating solar power systems. J Sol Energy Eng Jun. 2013;135(4):041007.

[23] sCO2-HeRo, "sCO2-HeRo project - the supercritical CO2 heat removal system." [Online]. Available: http://www.sco2-hero.eu/. [Accessed: 12-Feb-2018].

[24] Strätz M, Starflinger J, Mertz R, Seewald M, Schuster S, Brillert D. Cycle calculations of a small-scale heat removal system with supercritical CO2 as working fluid. In: Nuclear fuel and material, reactor physics and transport theory; innovative nuclear power plant design and new technology application, vol. 3; 2017, V003T13A001.

[25] Toshiba, "Toshiba : Press Release (1 Nov, 2016): Toshiba Ships Turbine for World's First Direct-Fired Supercritical Oxy-Combustion CO2 Power Cycle Demonstration Plant to U.S." [Online]. Available: https://www.toshiba.co.jp/about/press/2016_11/pr0101.htm. [Accessed: 12-Feb-2018].

[26] Huck P, Freund S, Lehar M, Peter M. Performance comparison of supercritical CO2 versus steam bottoming cycles for gas turbine combined cycle applications. In: 5th int. Symp. - sCO2 power Cycles2, vol. 1; 2016. p. 1–14.

[27] Cheang VT, Hedderwick RA, McGregor C. Benchmarking supercritical carbon dioxide cycles against steam rankine cycles for concentrated solar power. Sol Energy Mar. 2015;113:199–211.

[28] Miller JD, et al. Comparison of supercritical CO2 power cycles to steam Rankine cycles in coal-fired applications. In: ASME turbo expo 2017: turbo-machinery technical conference and exposition; 2017. p. 1–12.

[29] Dostal V, Hejzlar P, Driscoll MJ. The supercritical carbon dioxide power cycle: comparison to other advanced power cycles. Nucl Technol 2006;154(3):283–301.

[30] Echogen Power Systems, "Waste Heat Recovery Power Generation | Echogen Power Systems." [Online]. Available: https://www.echogen.com/. [Accessed: 12-Feb-2018].

[31] Persichilli M, Kacludis A, Zdankiewicz E, Held T. Supercritical CO 2 power cycle developments and commercialization: Why sCO 2 can displace steam steam. Asia: Power-Gen India Cent; 2012. p. 1–15.

[32] Kacludis A, Lyons S, Nadav D, Zdankiewicz E. Waste heat to power (WH2P) applications using a supercritical CO 2 -based power cycle. Power-Gen Int. 2012;2(December):1–10.

[33] Macchi E, Astolfi M. Axial flow turbines for Organic Rankine Cycle applications. In: Organic Rankine Cycle (ORC) power systems: technologies and applications. 1st Edition. Woodhead Publishing; 2016, ISBN 9780081005101. p. 299–319. https://doi.org/10.1016/B978-0-08-100510-1.00009-0.

[34] Astolfi M, Romano MC, Bombarda P, Macchi E. Binary ORC (Organic Rankine Cycles) power plants for the exploitation of medium-low temperature geothermal sources - Part B: techno-economic optimization. Energy Mar. 2014;66:435–46.

[35] Personal communication with industrial gas cooler manufacturer".

[36] MATLAB - MathWorks. The Mathworks Inc.; 2016 [Online]. Available: http://www.mathworks.com/products/matlab/.

[37] Lemmon EW, Huber ML, McLinden MO. NIST standard reference database 23. 2013. Reference Fluid Thermodynamic and Transport Properties (REFPROP), Version 9.1.

[38] Angelino G. Carbon dioxide condensation cycles for power production. J Eng Gas Turbines Power Jul. 1968;90(3):287.

[39] Ahn Y, et al. Cycle layout studies of S-CO 2 cycle for the next generation nuclear system application. In: Trans. Korean nucl. Soc. Autumn meet. Pyeongchang; 2014. p. 2–5.

[40] Astolfi M, Martelli E, Pierobon L. Thermodynamic and technoeconomic optimization of Organic Rankine Cycle systems. In: Organic Rankine Cycle (ORC) Power Systems: Technologies and applications. 1st Edition. Woodhead Publishing; 2016, ISBN 9780081005101. p. 173–249. https://doi.org/10.1016/B978-0-08-100510-1.00007-7.

[41] OpenEI, "Neal Hot Springs Geothermal Area | Open Energy Information." [Online]. Available: https://openei.org/wiki/Neal_Hot_Springs_Geothermal_ Area. [Accessed: 12-Feb-2018].

[42] Astolfi M, et al. Testing of a new supercritical ORC technology for efficient power generation from geothermal low temperature resources. In: Rotterdam: 2nd international seminar in ORC power systems; 2013.

[43] S. p. A. Exergy, "Binary cycle geothermal power plant | Organic Rankine Cycle Geothermal." [Online]. Available: http://exergy-orc.com/applications/geothermal. [Accessed: 12-Feb-2018].

[44] Zanellato L, Astolfi M, Serafino A, Rizzi D, Macchi E. Field performance evaluation of ORC geothermal power plants using radial outflow turbines. In: Energy procedia, vol. 129; 2017. p. 607–14.

[45] Astolfi M. Technical options for Organic Rankine Cycle systems. In: Organic Rankine Cycle (ORC) power systems: technologies and applications. 1st Edition. Woodhead Publishing; 2016, ISBN 9780081005101. p. 67–89. https://doi.org/10.1016/B978-0-08-100510-1.00003-X.